land

Article

Effects of *Dodonaea viscosa* Afforestation on Soil Nutrients and Aggregate Stability in Karst Graben Basin

Lijun Liu, Guanglin Gou, Jinxia Liu, Xuebin Zhang, Qilin Zhu, Jinxia Mou, Ruoyan Yang, Yunxing Wan, Lei Meng, Shuirong Tang, Yanzheng Wu and Qiuxiang He *

College of Tropical Crops, Hainan University, Haikou 570228, China; 20095132210020@hainanu.edu.cn (L.L.); 19095132210005@hainanu.edu.cn (G.G.); 20095132210019@hainanu.edu.cn (J.L.); 20095132210038@hainanu.edu.cn (X.Z.); 19090101110007@hainanu.edu.cn (Q.Z.); 21220951320021@hainanu.edu.cn (J.M.); 21220951320036@hainanu.edu.cn (R.Y.); 21210903000006@hainanu.edu.cn (Y.W.); menglei@hainanu.edu.cn (L.M.); srtang@hainanu.edu.cn (S.T.); 993741@hainanu.edu.cn (Y.W.)

* Correspondence: heqiuxiang@hainanu.edu.cn; Tel./Fax: +86-898-6627-9014

Abstract: *Dodonaea viscosa* is widely cultivated in the karst graben basin and is crucial for recovering land after rocky desertification. However, the effect of long–time *D. viscosa* afforestation on changes in the quality of soil remains unclear. Soil nutrients and aggregate composition can be used to evaluate the beneficial effects of afforestation of *D. viscosa* in improving soil functional stability. In this study, soil nutrients and aggregate stability were investigated using cropland, 10–year, 20–year, and 40–year *D. viscosa* afforestation and secondary succession shrub. Compared to the cropland, *D. viscosa* afforestation significantly increased the soil water content (WC), soil organic carbon (SOC), and total nitrogen (TN) contents, with an enhanced effect observed with prolonged afforestation. Soil nutrient contents under *D. viscosa* afforestation rapidly reached the level of the shrub. *Dodonaea viscosa* afforestation promoted the formation of >2 mm aggregates and decreased the ratio of 0.053–0.25 mm aggregates, which varied with afforestation years. Compared to the cropland, the content of >0.25 mm water–stable aggregates ($R_{>0.25}$), mean weight diameter (MWD), and geometric mean weight diameter (GMD) of soil increased exponentially. However, soil erodibility factor (K) and unstable aggregates index (E_{lt}) decreased exponentially with prolonged *D. viscosa* afforestation, and the latter two indicators did not reach the level of the shrub. These results indicated that soil nutrients, aggregate stability, and erosion resistance increased with prolonged *D. viscosa* afforestation. However, the aggregate stability and erosion resistance exhibited by *D. viscosa* could not reach the level of secondary shrub for a long time.

Keywords: karst graben basin; *Dodonaea viscosa*; soil nutrients; aggregate composition; aggregate stability

Citation: Liu, L.; Gou, G.; Liu, J.; Zhang, X.; Zhu, Q.; Mou, J.; Yang, R.; Wan, Y.; Meng, L.; Tang, S.; et al. Effects of *Dodonaea viscosa* Afforestation on Soil Nutrients and Aggregate Stability in Karst Graben Basin. *Land* **2022**, *11*, 1140. https://doi.org/10.3390/land11081140

Received: 26 May 2022
Accepted: 22 July 2022
Published: 25 July 2022

1. Introduction

Karst graben basin is a typical landform in southern China and is characterized by complex hydrology, climate, soil, geographical characteristics, and violently changing "basin to mountain" terrain [1–3]. It is associated with several ecological problems, such as poor vegetation, soil erosion, and rocky desertification, which seriously restrict the sustainable development of regional economies and society [4–6]. Considering the existing problems in the graben basin, the restoration of artificial vegetation in this region is promoted largely by selecting tree species [7,8]. However, the survival rate of plants is low due to the poor ecological adaptability and self–renewal ability of certain plants [9,10]. In addition, closed forests formed by artificial planting in certain regions in a short time turn into sparse forests or scattered trees over time [11], thereby continuously consuming soil nutrients, exerting a small effect on soil restoration, aggravating soil erosion and degradation, and slowing down the process of ecosystem restoration [12,13]. Depending on

the particularity of regional climate and geological conditions, cultivating suitable plants can significantly accelerate the ecological restoration of the karst graben basin [8,11,14]. *Dodonaea viscosa* is widely planted in the Yunnan graben basin for ecological restoration of rocky desertification due to its strong adaptability, tolerance to drought and barrenness, and ability to grow in conditions of topsoil erosion, rock exposed gravel soil, and rock crevices [14–16]. In addition, *D. viscosa* is involved in soil and water conservation, wind prevention, and sand fixation [13,17]. Numerous studies have been conducted recently to investigate the physiological characteristics [14,15], sediment interception capacity [13,17,18], and optimal afforestation density [14,19]. However, only a few studies exist on soil quality assessment. In addition, it is unknown whether the soil environment can be restored to the near–natural level after *D. viscosa* afforestation. Soil quality, as a comprehensive reflection of soil properties, can indicate dynamic changes in soil conditions and explain soil restoration or degradation [20,21].

Soil aggregates and nutrients are two important indicators for evaluating soil quality restoration [22,23]. Soil aggregates serve as the foundation of soil structure composition [23,24]. Their quantity distribution and spatial arrangement determine the distribution and continuity of soil pores, which can affect soil nutrient supply, soil structure stability, water holding capacity, permeability, and erosion resistance [13,17,25]. Soil aggregates with poor stability tend to disintegrate into fine particles, leading to soil leakage [13,23]. A good soil aggregate structure can enhance soil stability and reduce soil erosion [25,26]. Moreover, a high number of soil aggregates can improve soil porosity [17,24]. Loose and porous soil is conducive to the extension of plant roots, thereby increasing the aggregation of soil animals and microorganisms and continuously improving soil environmental conditions [23,26]. Soil nutrients contribute to ecosystem maintenance and stability because of their significant role in the element cycle, which not only affects the development and succession rate of the vegetation community but also notably impacts the ecosystem structure and productivity [20–22]. High soil nutrients are conducive to plant growth, thereby facilitating the restoration of soil functions [27,28]. Therefore, the study of soil aggregates and nutrients is essential for understanding and evaluating the restoration of ecosystem functions and contributes to advancing vegetation succession and accelerating artificial regulation of ecological restoration [23,29].

We selected *D. viscosa* with afforestation years of 0–year (cropland), 10–year, 20–year, and 40–year as the research objects, and the secondary succession shrub forest as the control to determine soil physicochemical properties and soil aggregate size distribution and stability to (1) explore the influence mechanism of *D. viscosa* afforestation on soil nutrients, aggregate distribution and stability, and (2) evaluate whether *D. viscosa* afforestation is conducive to improving soil functional stability and reaching the level of the secondary shrub. Finally, research findings can provide a theoretical basis for the restoration of rocky desertification in the graben basin.

2. Materials and Methods

2.1. Site Description and Soil Samples

The studied sample sites were located in the typical karst graben basin of Jianshui City, Yunnan Province, southwestern China (102°54′–102°56′ E, 23°36′–23°43′ N). As a typical karst landform, the topography is dominated by mountains and basins. The climate of the region is a typical subtropical monsoon. The average annual temperature is 18.5 °C, and the average annual precipitation is 805 mm, with 52% of the rainfall occurring between June and August. Annual evaporation is almost thrice the annual precipitation. The cropland was reclaimed from shrubs, and navel orange was planted continuously for 11 years with an annual fertilizer rate of 280 kg $N{\cdot}ha^{-1}$, 200 kg $P_2O_5{\cdot}ha^{-1,}$ and 160 kg $K_2O{\cdot}ha^{-1}$. The aboveground biomass in the cropland was removed through harvesting. A total of 3 *D. viscosa* afforestation ages of 10, 20, and 40 years were selected, all of which were converted from croplands. The main tree species of the shrub are *Pinus massoniana*, *Inula cappa*, *Osyris lanceolata*, *Ficus capensis*, *Bauhinia brachycarpa*, *Osteomeles schwerinae*, *Carex alopecuroides*, and

Carex parva Nees. The slope (approximately 7°) and altitude (approximately 1400–1500 m) were relatively consistent between the sites of cropland, *D. viscosa* afforestation, and shrub (Figure 1). The type of soil is calcareous Alfisoil (WRB Soil Taxonomy).

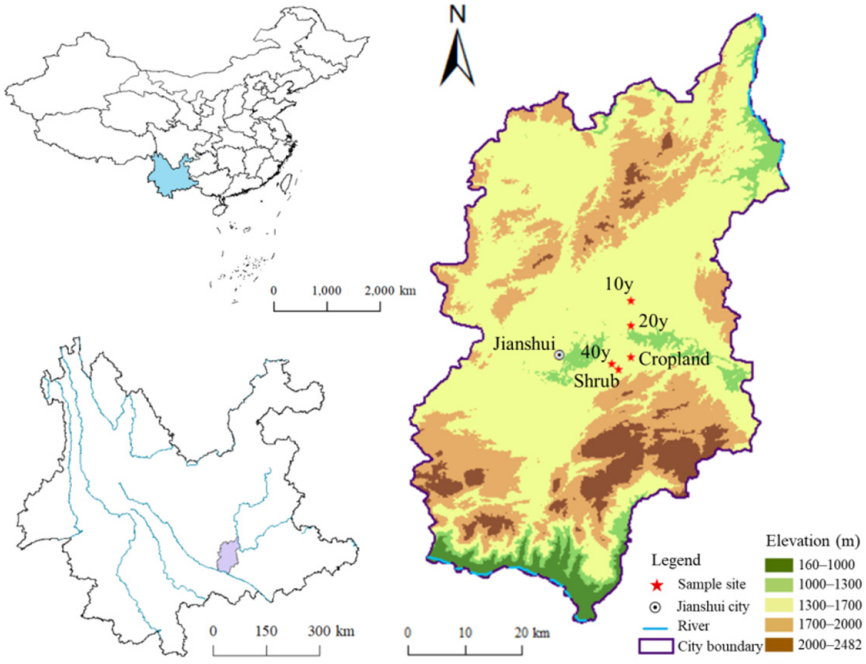

Figure 1. Location of the study area.

In August 2021, four representative sites were selected from cropland, *D. viscosa* with different afforestation years, and shrub as the spatial replicate. These shared the same soil type, aspect, slope, slope position, and elevation. A total of 3 plots (1 m × 1 m) were randomly selected at 20 m intervals for each site with a distance exceeding 300 m between different sites. Three soil cores (5 cm in diameter, 0–10 cm in depth) were collected from each sample plot, and subsequently, all subsamples were mixed into a composite sample. Soil samples were air–dried after removing stones and plant roots. Next, these were separated into two equal parts; one part was passed through a 2 mm sieve to determine the physical and chemical properties of soil, and the other part was used to measure the particle size distribution of soil aggregates.

2.2. Investigation of Soil Aggregate Stability

The wet sieving method was used to determine soil aggregate size distribution [26]. For this, 50 g of air–dried bulk soil (diameter less than 8 mm) was evenly placed in the uppermost layer of stacked sieves of 4, 2, 0.25, and 0.053 mm. The stacked sieves were placed into a cylindrical bucket containing deionized water. The water level in the bucket was adjusted so that the water surface completely covered the sample. After soaking for 10 min, the sieves were mechanically sieved for 30 min (amplitude of 3 cm, frequency of 25 times/min). The aggregates with different particle sizes remaining on every sieve were collected and transferred to aluminum boxes. Particles smaller than 0.053 mm were deposited in the bucket for 24 h. Next, the supernatant was discarded, and the soil samples were transferred to aluminum boxes. After drying at 60 °C to constant weight, the mass fractions of aggregates with diverse sizes were calculated. Finally, five particle components of 4–8 mm, 2–4 mm, 0.25–2 mm, 0.053–0.25 mm, and <0.053 mm were obtained.

Water–stable aggregate content (>0.25 mm) ($R_{>0.25}$), mean weight diameter (MWD), geometric mean weight diameter (GMD), fractal dimension (D), unstable aggregate index (E_{It}), and soil erodibility factor (K) were used to evaluate the stability of soil aggregates. The following formulae were used:

$R_{>0.25}$ indicates the quality of soil structure, and its quantity showed a positive correlation with soil fertility [30].

$$R_{>0.25} = \frac{M_{r>0.25}}{M_T} \times 100\% \quad (1)$$

Soil MWD and GMD are important evaluation indexes that reflect the aggregate distribution and stability. A large MWD value indicates a high content of aggregates with a large grain size and better water stability of aggregates. A higher geometric mean weight diameter indicates that the soil aggregates with large sizes are more distributed and have better porosity [31].

$$MWD = \sum_{i=1}^{n} x_i w_i \quad (2)$$

$$GMD = \exp(w_i \ln x_i) \quad (3)$$

Fractal dimension can better reveal the effect of water–stable aggregate content on soil structure and stability. A higher fractal dimension indicates higher soil clay content, finer soil texture, lower soil dispersion, and poor aggregate stability [17].

$$D = 3 - \frac{\lg\left(\frac{w_{(\delta < d_i)}}{w_0}\right)}{\lg\left(\frac{d_i}{d_{max}}\right)} \quad (4)$$

Soil unstable aggregate index (E_{It}) increased with the degree of soil degradation, which can better reflect the stability of soil structure [32].

$$E_{It} = \frac{M_T - M_{r>0.25}}{W_T} \times 100\% \quad (5)$$

The soil erodibility factor was found to be a vital indicator for assessing soil erosion and damage resistance and soil sensitivity to external erodibility. Its value was inversely proportional to soil erosion resistance [33].

$$K = 7.954 \times \left\{0.0017 + 0.0494 \times \exp\left[-0.5 \times \left(\frac{\lg GMD + 1.67}{0.6986}\right)^2\right]\right\} \quad (6)$$

where $M_{r>0.25}$ is the soil aggregate weight of wet sieve >0.25 mm (g), M_T represents the total weight of soil aggregates (g), X_i indicates the average diameter of soil aggregates with different sizes (mm), W_i indicates the mass percentage of soil aggregates with different particle sizes (%), d_{max} represents the mean diameter of the maximum particle size aggregate (mm), $w_{(}\delta < d_{i)}$ is the accumulated weight of soil diameter smaller than d_i (g), and w_0 is the sum of the weight of whole particle size aggregates (g).

2.3. Soil Physiochemical Analyses

Samples were dried in an oven at 105 °C for 24 h to measure the soil moisture content (WC). Soil pH was measured at a 1:2.5 (*w*:*v*) soil:water mixture using a DMP–2 mV/pH detector. After inorganic C was removed with 1 M HCl solution and washed to neutral with deionized water, soil organic carbon (SOC) and total nitrogen (TN) were measured by the Sercon Integra 2 element analyzer (Sercon Ltd., Crewe, UK). Soil total phosphorus (TP) and calcium (Ca) were measured by X-ray fluorescence spectrometry (XRF). NH_4^+ and NO_3^- in the soil were extracted with 2 M KCl at the soil–to–solution ratio of 1:5 and determined by a continuous flow analyzer (Skalar; Breda, The Netherlands). The ammonium acetate method was used to determine the cation–exchange capacity (CEC) of soils [34]. Soil samples (<2 mm) were pre–treated with hydrogen peroxide (H_2O_2) and hydrogen peroxide (HCl) to remove organic material and carbonates, respectively, and followed by adding the dispersed agent of sodium hydroxide (NaOH) for texture analyses. Subsequently, the samples were dispersed in an ultrasonic bath and the distribution of

particle size was measured by using a laser particle characterization analyzer (Beckman Coulter LS–230, Brea, CA, USA).

2.4. Data and Statistical Analyses

Statistical analyses were performed using Microsoft Excel 2010 and SPSS 19.0 software. The discrepancy in soil properties, aggregate particle size distribution, and stability at $p < 0.05$ were assessed by one–way analysis of variance (ANOVA) and least square difference (LSD) multiple comparison test. A bivariate test was used to evaluate the relationship between soil physicochemical properties, aggregate size distribution, and stability characteristics. Pearson correlation analysis was used to evaluate the relationship between afforestation years, soil physicochemical properties, and aggregate stability. The Origin 2021 Pro was used for plotting, and the data in the chart represent mean ± standard deviation.

3. Results

3.1. Soil Physicochemical Properties

Compared with the cropland, *D. viscosa* afforestation significantly increased SOC, TN, TP, Ca, NH_4^+, and NO_3^- contents, and pH and CEC (Table 1). Soil nutrient content under *D. viscosa* afforestation reached the level of the shrub in different periods. WC, SOC, and TN contents increased with the extension in afforestation years. NO_3^- content and pH declined with the duration of afforestation years. WC and NO_3^- content significantly differed with *D. viscosa* afforestation years ($p < 0.05$). There were no distinct differences in NH_4^+ content and CEC with prolonged afforestation years. The ratio of silt remained unchanged in *D. viscosa* afforestation, and the proportion of clay and sand declined and increased with the extension in afforestation years, respectively.

Table 1. Changes in physicochemical properties in soils with different afforestation years of *D. viscosa*.

Parameter [i]	Cropland	10 y [ii]	20 y	40 y	Shrub
WC (%)	0.19 ± 0.02c	0.24 ± 0.04c	0.30 ± 0.04b	0.40 ± 0.04a	0.39 ± 0.01a
SOC (g C kg^{-1})	9.33 ± 0.24c	40.8 ± 4.84b	59.4 ± 7.64a	66.2 ± 6.05a	64.1 ± 2.73a
TN (g N kg^{-1})	0.69 ± 0.02c	3.31 ± 0.33b	4.67 ± 0.63a	5.15 ± 0.45a	5.22 ± 0.23a
pH	5.52 ± 0.02d	7.53 ± 0.12a	7.44 ± 0.17a	6.90 ± 0.13b	6.61 ± 0.12c
Clay (<2 μm) (%)	22.7 ± 1.53a	20.9 ± 1.94a	19.5 ± 1.92ab	15.9 ± 2.97bc	13.5 ± 1.96c
Silt (2–50 μm) (%)	56.8 ± 5.54a	57.4 ± 7.08a	56.5 ± 6.32a	57.3 ± 4.48a	53.8 ± 6.10a
Sand (50–2000 μm) (%)	20.6 ± 1.90c	21.8 ± 2.53c	24.0 ± 0.88bc	26.9 ± 2.17b	32.7 ± 4.26a
TP ($g \cdot kg^{-1}$)	0.61 ± 0.04c	0.74 ± 0.04b	0.93 ± 0.10a	0.84 ± 0.06ab	0.79 ± 0.05b
Ca ($g \cdot kg^{-1}$)	3.55 ± 0.12c	10.9 ± 1.32b	13.7 ± 2.71a	10.7 ± 0.98b	9.65 ± 0.79b
NH_4^+ (mg $N \cdot kg^{-1}$)	4.31 ± 0.54b	16.8 ± 0.26a	18.3 ± 0.54a	18.5 ± 3.57a	16.0 ± 4.56a
NO_3^- (mg $N \cdot kg^{-1}$)	7.73 ± 1.05d	21.6 ± 1.38a	19.4 ± 1.76b	16.4 ± 0.47c	8.77 ± 1.20d
CEC ($cmol \cdot kg^{-1}$)	15.9 ± 1.53b	26.3 ± 1.57a	27.1 ± 0.61a	28.5 ± 1.03a	28.7 ± 1.59a

[i] WC, water content; SOC, soil organic carbon; TN, total N; TP, total P; CEC, cation exchange capacity. [ii] 10, 20, and 40 years represent the afforestation ages of *D. viscosa* after cropland returning. The same lowercase letters suggest no significant difference between different afforestation years of *D. viscosa* and shrub at 0.05 level.

3.2. Soil Aggregate Size Distribution

The variation ranges of <0.053 mm, 0.053–0.25 mm, 0.25–2 mm, 2–4 mm, and 4–8 mm particles were 10–21%, 6–28%, 40–50%, 5–18%, and 0–26%, respectively (Figure 2). The particles in the cropland were dominated by the size of <2 mm, and the percentage of aggregates in >2 mm was less than 6%. The size of soil aggregates in different afforestation years of *D. viscosa* ranged mainly from 0.25 to 2 mm. After *D. viscosa* afforestation, the percentage of soil aggregates in >2 mm increased by 279% to 467% compared with cropland; however, these were significantly lower than that of shrub ($p < 0.05$). *Dodonaea viscosa* afforestation did not significantly change the ratio of soil particles in 0.25–2 mm and <0.053 mm. The proportion of >2 mm aggregates and 0.053–0.25 mm aggregates in soils increased and decreased with the duration of afforestation years, respectively.

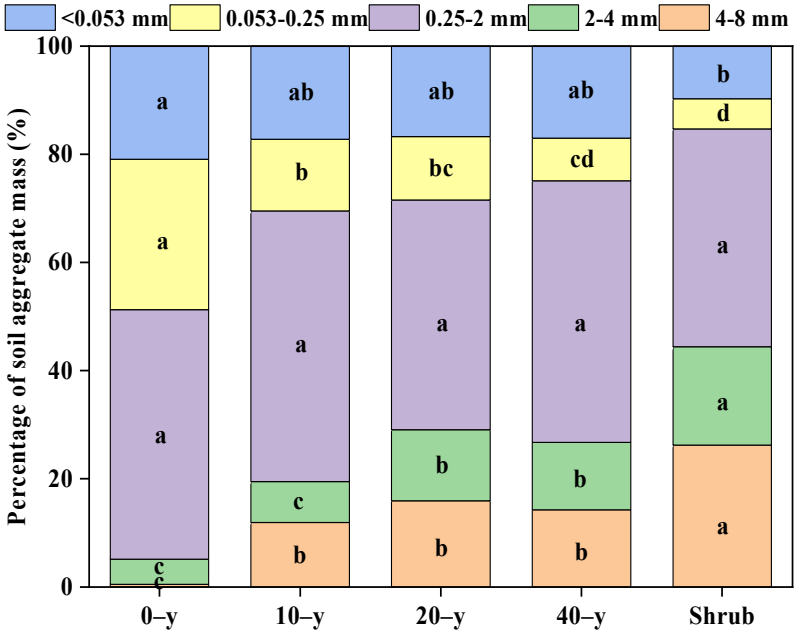

Figure 2. The size distribution of soil aggregates. Different lowercase letters indicate that soil aggregates with the same size reached the significance level of 0.05 between different afforestation years of *D. viscosa* and shrub.

3.3. Soil Aggregate Stability

Soil structure quality and aggregate stability of *D. viscosa* afforestation were significantly higher than those of the cropland and lower than those of shrub (indexes including $R_{>0.25}$, GMD, MWD, D and E_{It}, Table 2). *Dodonaea viscosa* afforestation substantially enhanced the soil erosion resistance ability compared with the cropland (Index K). There were no significant changes in soil structure quality, aggregate stability, and soil erosion resistance ability with different afforestation years ($p > 0.05$).

Table 2. Stability characteristics of soil aggregate.

Parameter [i]	Cropland	10 y	20 y	40 y	Shrub
$R_{>0.25}$ (%)	51.3 ± 10.1c	69.5 ± 3.24b	71.5 ± 3.24b	75.1 ± 6.86ab	84.7 ± 3.95a
MWD (mm)	73.6 ± 13.9c	153 ± 15.4b	185 ± 26.8b	179 ± 12.6b	258 ± 38.9a
GMD (mm)	0.33 ± 0.13c	0.60 ± 0.08bc	0.71 ± 0.12b	0.75 ± 0.17b	1.34 ± 0.32a
D	2.98 ± 0.01a	2.56 ± 0.09b	2.39 ± 0.18b	2.46 ± 0.07b	1.93 ± 0.36c
K	0.12 ± 0.04a	0.06 ± 0.01b	0.05 ± 0.01b	0.05 ± 0.01b	0.03 ± 0.01b
E_{It} (%)	48.7 ± 10.1a	30.5 ± 3.24b	28.5 ± 3.24b	24.9 ± 6.86bc	15.3 ± 3.95c

[i] $R_{>0.25}$, >0.25 mm water–stable aggregate content; MWD, mean weight diameter; GMD, geometric mean weight diameter; D, fractal dimension; K, soil erodibility factor; E_{It}, unstable aggregate index. The same lowercase letters suggest no significant difference between different afforestation years of *D. viscosa* and shrub at 0.05 level.

3.4. Relationship between Soil Physicochemical Properties and Soil Aggregate Stability

Strong interactions existed between soil properties, aggregate distribution, and stability and erosion resistance ability (Table 3). High SOC, TN, and Ca contents were conducive to the formation of soil aggregates in 2–4 mm and 4–8 mm. Soil aggregates stability (indexes including $R_{>0.25}$, GMD, MWD, D, and E_{It}) and erosion resistance ability (index K) increased with soil SOC, TN, and Ca contents. The ratios of sand and clay were closely related to soil aggregate composition (2–8 mm and 0.053–0.25 mm) and stability. A high proportion of sand and a low proportion of clay can enhance soil aggregate stability and erosion resistance.

Table 3. Correlation between soil physicochemical properties and soil aggregate size distribution and stability.

	WC	SOC	TN	pH	Clay	Silt	Sand	TP	Ca	NH_4^+	NO_3^-	CEC
MWD	0.691 **	0.798 **	0.816 **	0.493 *	−0.593 **	−0.245	0.711 **	0.486 *	0.566 **	0.744 **	0.151	0.807 **
$R_{>0.25}$	0.695 **	0.825 **	0.848 **	0.470 *	−0.751 **	−0.093	0.748 **	0.565 **	0.605 **	0.696 **	0.094	0.813 **
GMD	0.615 **	0.659 **	0.687 **	0.234	−0.703 **	−0.193	0.817 **	0.341	0.355	0.545 *	−0.145	0.658 **
D	−0.614 **	−0.751 **	−0.777 **	−0.413	0.759 **	0.047	−0.705 **	−0.526 *	−0.559 *	−0.571 **	−0.052	−0.748 **
K	−0.661 **	−0.794 **	−0.809 **	−0.592 **	0.544 *	0.245	−0.595 **	−0.505 *	−0.636 **	−0.758 **	−0.268	−0.830 **
E_{It}	−0.691 **	−0.798 **	−0.816 **	−0.493 *	0.593 **	0.245	−0.711 **	−0.486 *	−0.566 **	−0.744 **	−0.151	−0.807 **
4–8 mm	0.642 **	0.791 **	0.816 **	0.466 *	−0.759 **	−0.046	0.705 **	0.565 **	0.608 **	0.628 **	0.105	0.787 **
2–4 mm	0.743 **	0.774 **	0.790 **	0.322	−0.700 **	−0.062	0.763 **	0.515 *	0.475 *	0.741 **	−0.040	0.701 **
0.25–2 mm	−0.157	−0.186	−0.200	0.035	0.471 *	−0.350	−0.223	−0.264	−0.140	−0.036	0.170	−0.107
0.053–0.25 mm	−0.740 **	−0.911 **	−0.923 **	−0.634 **	0.656 **	0.051	−0.671 **	−0.670 **	−0.719 **	−0.823 **	−0.325	−0.895 **
<0.053 mm	−0.400	−0.394	−0.412	−0.157	0.319	0.399	−0.522 *	−0.098	−0.191	−0.400	0.112	−0.430

* $p < 0.05$; ** $p < 0.01$.

3.5. Relationship between Afforestation Years and Soil Aggregate Stability

Soil aggregate stability and erosion resistance ability significantly varied with *D. viscosa* afforestation (Figure 3). *Dodonaea viscosa* afforestation increased exponentially with $R_{>0.25}$, MWD, and GMD and decreased exponentially with D, K, and E_{It}. This result indicates that soil aggregate stability and erosion resistance ability enhanced exponentially with increased afforestation years and still did not reach the level of the shrub.

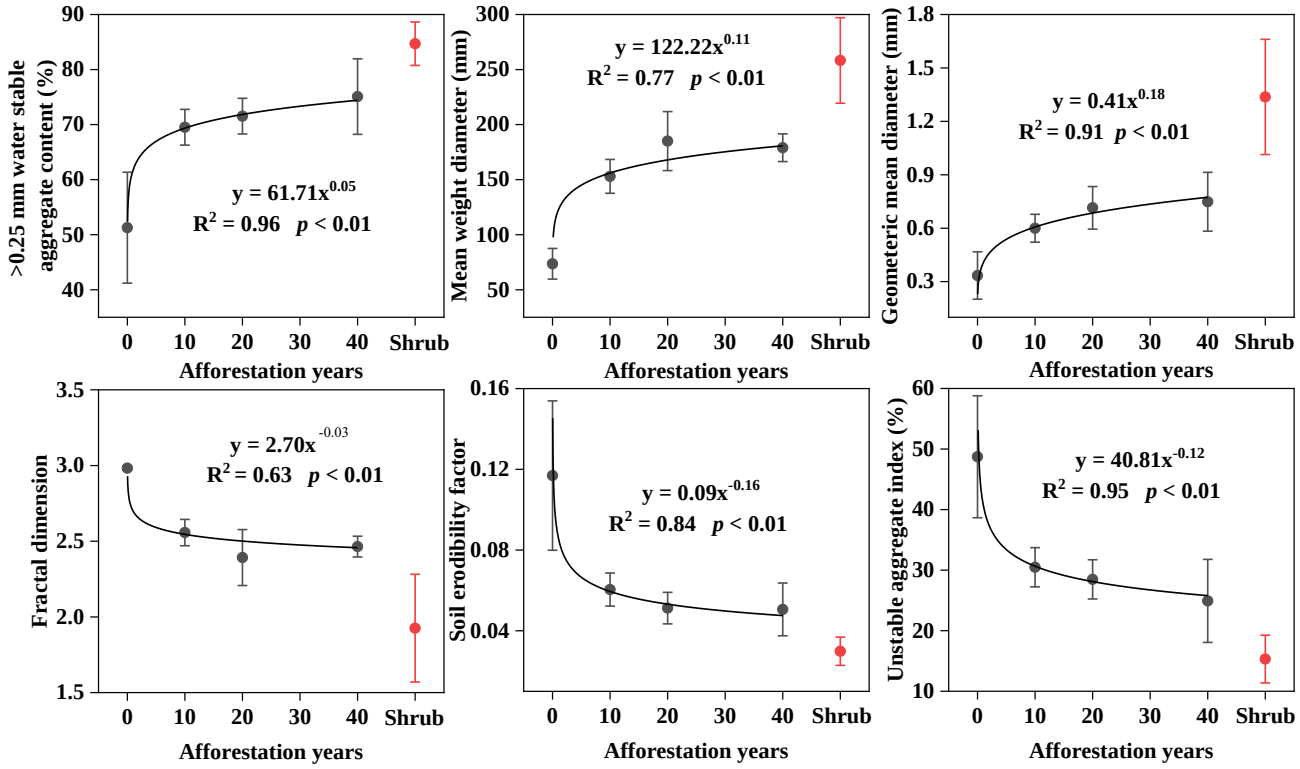

Figure 3. Relationship between soil aggregate stability characteristics and afforestation years.

3.6. Correlation between Afforestation Years and Soil Properties and Aggregate Stability

Soil properties and soil aggregate stability and erosion resistance ability were found to be closely associated with the afforestation years of *D. viscosa* (Table 4). The positive correlation between afforestation years and WC, SOC, TN, sand, TP, NH_4^+, CEC, MWD, $R_{>0.25}$, and GMD was highly significant ($p < 0.01$). The NO_3^-, pH, and silt were unaffected by afforestation years. A significant and negative correlation existed between afforestation years and D, clay, K, and E_{It} ($p < 0.05$).

Table 4. Correlation between afforestation years and soil nutrients and soil aggregate stability.

Soil Nutrients		Stability Characteristics of Soil Aggregates	
Parament	**Correlation Coefficient**	**Parameter**	**Correlation Coefficient**
WC	0.906 **	MWD	0.724 **
SOC	0.870 **	$R_{>0.25}$	0.674 **
TN	0.859 **	GMD	0.678 **
pH	0.430	D	−0.662 **
Clay	−0.757 **	K	−0.612 *
Silt	0.016	E_{It}	−0.674 *
Sand	0.770 **		
TP	0.634 **		
Ca	0.541 *		
NH_4^+	0.713 **		
NO_3^-	0.372		
CEC	0.766 **		

* $p < 0.05$; ** $p < 0.01$.

4. Discussion

4.1. Effects of Dodonaea viscosa Afforestation on Soil Physiochemical Properties

Vegetation recovery can significantly increase litter quantity, root biomass, and exudates, which is conducive to the accumulation of soil nutrients [14,35,36]. Previous studies have reported that soil organic C, N, and phosphorus are the primary nutrients that can affect the success of afforestation [22,29]. In this study, *D. viscosa* afforestation notably increased soil nutrient content and reached the level of the shrub (Table 1), indicating that nutrients can reach near–natural levels after afforestation in karst areas. The contents of SOC, TN, and TP significantly increased under *D. viscosa* afforestation, which ensured the nutrient supply for aboveground plants [7–10]. In addition, physical entanglement of plant roots with soil particles can increase soil permeability with the duration of afforestation, which is conducive to enhancing soil microbial growth and activities and facilitating soil nutrient cycling [20,27,37]. Soil moisture, as an important source of water absorption by plants, plays a crucial role in vegetation growth and restoration [7,16,20]. Our results showed that soil water content increased with prolonged afforestation years (Table 1). Favorable water conditions can promote the transport of soil nutrients in plants and enhance microbial activity, thus significantly affecting the stability and sustainable development of regional ecosystems [8,29].

4.2. Effects of Dodonaea viscosa Afforestation on the Soil Aggregates Size Distribution and Stability

Aggregate, the basic unit of soil structure, and its stability are a comprehensive reflection of the physical properties of soil [24–26]. Increasing evidence has verified that the main aggregates in the cropland had a small particle size, and the overall stability of soil aggregates was at a low level [24,31,38]. This phenomenon could be attributed to the high frequency and intensity of tillage and few inputs of plant residues due to the regular removal of aboveground biomass in the cropland [30,31,33,39]. Our results indicated that soil aggregates in the cropland were less stable. This may be due to tillage destructed plant roots and reduced stability of plant root fibers, which were not conducive to soil agglomeration [33,39]. In addition, the proportion of >2 mm aggregates in the cropland was extremely low. The large–size aggregates are relatively more susceptible to the disruptive forces of tillage because of the presence of fewer stable binding agents than small–size aggregates [40]. Our results also suggested that *D. viscosa* afforestation affected the transformation and redistribution of soil aggregates in 0.053–0.25 mm and >2 mm and facilitated the recovery of soil aggregate stability and erosion resistance ability. Soil aggregate stability and erosion resistance ability were closely related to soil properties and vegetation restoration [23,24,26]. Studies confirmed that the soil developed from carbonate rock in the karst region has the characteristics of low content of acid–insoluble matter, high pH, and high calcium (Ca) content [41,42]. Soil organic matter (SOM) can interact

with Ca to facilitate the formation of large–size aggregates, which is an important reason for the formation of >2 mm aggregates in *D. viscosa* afforestation [43]. Meanwhile, soil agglomeration increased with microbial activities in high substrates, as the secretion of microorganisms can act as organic binding agents [37]. Vegetation restoration can improve soil coverage and weaken water erosion, reducing the loss of soil particles [22,31]. The high molecular viscosity produced by plant root exudates exerted a strong adhesive force on soil particles [30,44]. The decrease in anthropogenic disturbance favored the interaction between soil and plant roots during vegetation recovery, thus increasing the stability of soil aggregates [30,31,45].

Previous studies have reported that natural vegetation restoration was more beneficial to soil agglomeration than monoculture plantation, which was in line with our study [42]. Our result manifested in the transformation of soil particles in <0.053 mm into >2 mm in the soil of shrub. The litter layer (2–3 cm) and the humus layer (2–3 cm) in the shrub were thicker, and the litter layer in the single *D. viscosa* afforestation was thinner (about 1 cm). Higher plant species diversity and coverage, litter quantity, root exudates, more developed root system, and longer recovery age of most tree species in the shrub can enhance soil heterogeneity and increase microbial diversity [30,44,46]. These differences may be caused by strong soil agglomeration in the shrub. In this study, *D. viscosa* afforestation induced the formation of >2 mm aggregates to improve soil structure; however, the stability of soil aggregates and erosion resistance ability did not reach the level of the shrub.

4.3. Relationship between Soil Physical and Chemical Properties and Soil Aggregate Stability

Changes in the environment and vegetation types can influence the distribution and stability of soil aggregates, affecting the soil nutrient content and its supply capacity [21,33,44,47]. Previous studies have found that the soil cohesiveness of fine particles can maintain the content of C and N [36,48]. In our study, soil aggregates of 0.053–0.25 mm and 2–8 mm were more sensitive than other particles along with vegetation restoration. The contents of SOC and TN were significantly positively correlated with 2–8 mm aggregates and negatively correlated with 0.053–0.25mm aggregates, respectively, indicating that vegetation recovery can facilitate the formation of large–size aggregates and, thus, physically protect SOM from microbial attack and mineralization [49,50]. Meanwhile, Ca can act as a polyvalent cation bridge between SOM and mineral surfaces [22,51]. Strong positive correlations of SOC, TN, and Ca with soil aggregate stability and erosion resistance ability (index $R_{>0.25}$, MWD, GMD, D, K, and E_{It}) were observed in our study. Their effective combination proved their important role in the increase in soil aggregates stability under afforestation. In addition, the other soil nutrients (e.g., TP and NH_4^+) increased with the ratio of aggregates in >2 mm, further suggesting that the formation of large–size aggregates provided a protective mechanism and reservoir for different nutrients [47,52]. Except for large–size aggregates, soil texture also has a close relationship with soil nutrients (e.g., SOC, TN, and NH_4^+) [53]. In our study, the portion of sand in soils showed a consistent trend with nutrient content, which indicated that a better soil structure and stronger soil erosion resistance could promote the maintenance of soil nutrients. The soil nutrient and aggregate results showed that the soil environment could be improved effectively by *D. viscosa* afforestation in the rocky desertification area of the graben basin. Soil nutrient content can reach the level of shrub and reduce the possibility of soil loss and erosion.

5. Conclusions

Compared with the cropland, WC, SOC, TN, and other nutrients were increased by different degrees following *D. viscosa* afforestation. Soil nutrient content under *D. viscosa* afforestation reached the level of the shrub at different periods. In addition, *D. viscosa* afforestation promoted the formation of >2 mm aggregates and decreased the ratio of 0.053–0.25 aggregates. Compared with the cropland, $R_{>0.25}$, MWD, and GMD increased, whereas D, K, and E_{It} reduced; however, the degree of change was less than that of secondary shrubs. With the extension of afforestation years, soil nutrient content increased,

and soil aggregate stability increased exponentially. *Dodonaea viscosa* afforestation restored soil nutrients and stabilized soil aggregates; however, the stability of soil aggregates was difficult to reach the level of the shrub. Taken together, *D. viscosa* afforestation can effectively improve the soil environment in the rocky desertification area of the graben basin and can be used as an effective species to reconstruct the degraded ecosystem in the karst area.

Author Contributions: Conceptualization, L.L., G.G., Q.Z. and Q.H.; Investigation, L.L., S.T. and Y.W. (Yanzheng Wu); Formal Analysis, L.L., G.G., J.L., X.Z., J.M., R.Y. and Y.W. (Yunxing Wan); Writing—Review and Editing, L.L., Q.Z., L.M. and Q.H. All authors have read and agreed to the published version of the manuscript.

Funding: This work was funded by the National Natural Science Foundation of China (42067008), The High-level Talent Project of the Natural Science Foundation of Hainan Province (320RC493).

Institutional Review Board Statement: Not applicable.

Informed Consent Statement: Not applicable.

Data Availability Statement: Not applicable.

Conflicts of Interest: The authors declare no conflict of interest.

References

1. Qiu, J.M.; Cao, J.H.; Lan, G.Y.; Liang, Y.M.; Wang, H.; Li, Q. The Influence of land use patterns on soil bacterial community structure in the karst graben basin of Yunnan province, China. *Forests* **2020**, *11*, 51. [CrossRef]
2. Lan, G.Y.; Liu, C.; Wang, H.; Tang, W.; Wu, X.; Yang, H.; Tu, L.L.; Hu, B.X.; Cao, J.H.; Li, Q. The effect of land use change and soil redistribution on soil organic carbon dynamics in karst graben basin of China. *J. Soils Sediments* **2021**, *21*, 2511–2524. [CrossRef]
3. Yang, H.; Zhang, P.; Zhu, T.B.; Li, Q.; Cao, J.H. The characteristics of Soil C, N, and P stoichiometric ratios as affected by geological background in a karst graben area, southwest China. *Forests* **2019**, *10*, 601. [CrossRef]
4. Green, S.M.; Dungait, J.A.J.; Tu, C.L.; Buss, H.L.; Sanderson, N.; Hawkes, S.J.; Xing, K.X.; Yue, F.J.; Hussey, V.L.; Peng, J.; et al. Soil functions and ecosystem services research in the Chinese karst Critical Zone. *Chem. Geol.* **2019**, *527*, 119107. [CrossRef]
5. Wang, S.J.; Liu, Q.M.; Zhang, D.F. Karst rocky desertification in southwestern China: Geomorphology, landuse, impact and rehabilitation. *Land Degrad. Dev.* **2010**, *15*, 115–121. [CrossRef]
6. Jiang, Z.C.; Lian, Y.Q.; Qin, X.Q. Rocky desertification in Southwest China: Impacts, causes, and restoration. *Earth Sci. Rev.* **2014**, *132*, 1–12. [CrossRef]
7. Zhang, Y.H.; Xu, X.L.; Li, Z.W.; Xu, C.H.; Luo, W. Improvements in soil quality with vegetation succession in subtropical China karst. *Sci. Total Environ.* **2021**, *775*, 145876. [CrossRef]
8. Shen, J.C.; Zhang, Z.H.; Liu, R.; Wang, Z.H. Ecological restoration of eroded karst utilizing pioneer moss and vascular plant species with selection based on vegetation diversity and underlying soil chemistry. *Int. J. Phytoremediat.* **2019**, *20*, 1–11. [CrossRef]
9. Gebretsadik, W.; Center, D.Z.A. Evaluation of the adaptability and response of indigenous trees to assisted rehabilitation on the degraded hillsides of Kuriftu Lake Catchment (Debre Zeit, Ethiopia). *J. For. Res.* **2014**, *25*, 97–102. [CrossRef]
10. Liu, C.N.; Huang, Y.; Wu, F.; Liu, W.J.; Ning, Y.Q.; Huang, Z.R.; Tang, S.Q.; Liang, Y. Plant adaptability in karst regions. *J. Plant Res.* **2021**, *134*, 1–18. [CrossRef]
11. Peng, S.; Chen, A.Q.; Fang, H.D.; Wu, J.L.; Liu, G.C. Effects of vegetation restoration types on soil quality in Yuanmou dry–hot valley, China. *Soil Sci. Plant. Nutr.* **2013**, *59*, 347–360. [CrossRef]
12. Jagger, P.; Pender, J. The role of trees for sustainable management of less-favored lands: The case of eucalyptus in Ethiopia. *For. Policy Econ.* **2003**, *5*, 83–95. [CrossRef]
13. Zhao, Y.Y.; Duan, X.; Han, J.J.; Yang, K.; Xue, Y. The main influencing factors of soil mechanical characteristics of the gravity erosion environment in the dry-hot valley of Jinsha river. *Open Chem.* **2018**, *16*, 796–809. [CrossRef]
14. Wang, G.Z.; Tang, G.Y.; Pang, D.B.; Liu, Y.G.; Wan, L.; Zhou, J.X. Plant inertactions control the carbon distribution of *Dodonaea viscosa* in karst regions. *PLoS ONE* **2021**, *16*, 260337. [CrossRef]
15. Afzal, I.; Iqrar, I.; Shinwari, Z.K.; Yasmin, A. Plant growth-promoting potential of endophytic bacteria isolated from roots of wild *Dodonaea viscosa* L. *Plant Growth Regul.* **2017**, *81*, 399–408. [CrossRef]
16. Pei, J.; Yang, W.; Cai, Y.P.; Yi, Y.J.; Li, X.X. Relationship between vegetation and environment in an arid-hot valley in southwestern China. *Sustainability* **2018**, *10*, 4774. [CrossRef]
17. Cui, Y.; Li, J.; Chen, A.M.; Wu, J.Z.; Luo, Q.H.; Rafay, L.; He, J.W.; Liu, Y.; Wang, D.J.; Lin, Y.M.; et al. Fractal dimensions of trapped sediment particle size distribution can reveal sediment retention ability of common plants in a dry-hot valley. *Catena* **2019**, *180*, 252–262. [CrossRef]
18. Majed, A. Factors affecting sediment trapping in vegetated filter strips: Simulation study using VFSMOD. *Hydrol Process.* **2001**, *15*, 1477–1488.

19. Zhang, W.P.; Xin, J.; Morris, E.C.; Bai, Y.Y.; Wang, G.X. Stem, branch and leaf biomass–density relationships in forest communities. *Ecol. Res.* **2012**, *27*, 819–825. [CrossRef]
20. Bünemann, E.K.; Bongiorno, G.; Bai, Z.G.; Creamer, R.E.; Deyn, G.D.; Goede, R.D.; Fleskens, L.; Geissen, V.; Kuyper, Y.W.; Mäder, P.; et al. Soil quality–A critical review. *Soil Biol. Biochem.* **2018**, *120*, 105–125. [CrossRef]
21. Arshad, M.A.; Coen, G.M. Characterization of soil quality: Physical and chemical criteria. *Am. J. Altern. Agric.* **1992**, *7*, 25–31. [CrossRef]
22. Lan, J.C.; Hu, N.; Fu, W.L. Soil carbon–nitrogen coupled accumulation following the natural vegetation restoration of abandoned farmlands in a karst rocky desertification region. *Ecol. Eng.* **2020**, *158*, 106033. [CrossRef]
23. Singh, S.; Singh, J.S. Water-stable aggregates and associated organic matter in forest, savanna, and cropland soils of a seasonally dry tropical region, India. *Biol. Fertil. Soils* **1996**, *22*, 76–82. [CrossRef]
24. Liu, M.; Han, G.; Zhang, Q. Effects of soil aggregate stability on soil organic carbon and nitrogen under land use change in an erodible region in southwest China. *Int. J. Environ. Res. Public Health* **2019**, *16*, 3809. [CrossRef] [PubMed]
25. Robot, E.; Wiesmeter, M.; Schlüter, S.; Vogel, H.J. Soil structure as an indicator of soil functions: A review. *Geoderma* **2018**, *314*, 122–137. [CrossRef]
26. Liu, M.Y.; Chang, Q.R.; Qi, Y.B.; Liu, J.; Chen, T. Aggregation and soil organic carbon fractions under different land uses on the tableland of the Loess Plateau of China. *Catena* **2014**, *115*, 19–28. [CrossRef]
27. Cheeke, T.E.; Schneider, M.; Saify, A.; Brauner, M.; Bunn, R. Role of soil biota in grassland restoration in high nutrient soils. *Restor. Ecol.* **2021**, *5*, 13549. [CrossRef]
28. Ordonez, J.C.; Bodegom, P.M.V.; Witte, J.P.M.; Wright, I.J.; Reich, P.B.; Aerts, R. A global study of relationships between leaf traits, climate and soil measures of nutrient fertility. *Glob. Ecol. Biogeogr.* **2010**, *18*, 137–149. [CrossRef]
29. Zhu, M.K.; Yang, S.Q.; Ai, S.H.; Ai, X.Y.; Jiang, X.; Chen, J.; Li, R.R.; Ai, Y.W. Artificial soil nutrient, aggregate stability and soil quality index of restored cut slopes along altitude gradient in southwest China. *Chemosphere* **2020**, *246*, 125687. [CrossRef]
30. Tisdall, J.M.; Oades, J.M. Organic matter and water-stable aggregates in soils. *Eur. J. Soil Biol.* **1982**, *33*, 141–163. [CrossRef]
31. Dou, Y.; Yang, Y.; An, S.; Zhu, Z. Effects of different vegetation restoration measures on soil aggregate stability and erodibility on the Loess Plateau, China. *Catena* **2020**, *185*, 104294. [CrossRef]
32. Liu, Z. Effect of long-term various organic materials incorporation on characteristics of soil quality and crop yield. *IOP Conf. Ser. Earth Environ. Sci.* **2018**, *170*, 22086. [CrossRef]
33. Lan, J.C. Changes of soil aggregate stability and erodibility after cropland conversion in degraded karst region. *J. Soil Sci. Plant. Nutr.* **2021**, *21*, 3333–3345. [CrossRef]
34. Ross, D.S.; Ketterings, Q. Recommended methods for determining soil cation exchange capacity. In *Recommended Soil Testing Procedures for the Northeastern United States*; University of Delaware Newark: Newark, DE, USA, 1995; pp. 62–70.
35. Liang, Y.M.; Pan, F.J.; He, X.Y.; Chen, X.B.; Su, Y.R. Effect of vegetation types on soil arbuscular mycorrhizal fungi and nitrogen-fixing bacterial communities in a karst region. *Environ. Sci. Pollut. Res.* **2016**, *23*, 18482–18491. [CrossRef] [PubMed]
36. Zhang, P.P.; Zhang, Y.L.; Jia, J.C.; Cui, Y.X.; Wang, X.; Zhang, Y.J.; Zhang, X.C.; Wang, Y.Q. Soil aggregation and aggregate-associated organic C and total N as affected by revegetation pattern at a surface mine on the Loess Plateau, China. *Soil Sci. Soc. Am. J.* **2019**, *83*, 388–397. [CrossRef]
37. Six, J.; Bossuyt, H.; Degryze, S.; Denef, K. A history of research on the link between (micro) aggregates, soil biota, and soil organic matter dynamics. *Soil Tillage Res.* **2004**, *79*, 7–31. [CrossRef]
38. Six, J.; Elliott, E.T.; Paustian, K. Soil macroaggregate turnover and microaggregate formation: A mechanism for C sequestration under no–tillage agriculture. *Soil Biol. Biochem.* **2000**, *32*, 2099–2103. [CrossRef]
39. Bronick, C.J.; Lal, R. Soil structure and management: A review. *Geoderma* **2005**, *124*, 3–22. [CrossRef]
40. Cambardella, C.A.; Elliott, E.T. Carbon and nitrogen dynamics of soil organic matter fractions from cultivated grassland soils. *Soil Sci. Soc. Am. J.* **1994**, *58*, 123–130. [CrossRef]
41. Yang, L.Q.; Luo, P.; Wen, L.; Li, D.J. Soil organic carbon accumulation during post-agricultural succession in a karst area, southwest China. *Sci. Rep.* **2016**, *6*, 637118. [CrossRef]
42. Lan, J.C.; Long, Q.X.; Huang, M.Z.; Jiang, Y.X.; Hu, N. Afforestation-induced large macroaggregate formation promotes soil organic carbon accumulation in degraded karst area. *For. Ecol. Manag.* **2022**, *505*, 119884. [CrossRef]
43. Fernández–Ugalde, O.; Virto, I.; Barré, P.; Gartzia–Bengoetxea, N.; Enrique, A.; Imaz, M.J.; Bescansa, P. Effect of carbonates on the hierarchical model of aggregation in calcareous semi–arid Mediterranean soils. *Geoderma* **2011**, *164*, 203–214. [CrossRef]
44. Wei, X.R.; Li, X.Z.; Jia, X.X.; Shao, M.G. Accumulation of soil organic carbon in aggregates after afforestation on abandoned farmland. *Biol. Fertil. Soils* **2013**, *49*, 637–646. [CrossRef]
45. Tang, F.K.; Cui, M.; Lu, Q.; Liu, Y.G.; Guo, H.Y.; Zhou, J.X. Effects of vegetation restoration on the aggregate stability and distribution of aggregate–associated organic carbon in a typical karst gorge region. *Solid Earth Discuss.* **2016**, *7*, 2213–2242. [CrossRef]
46. Ilay, R.; Kavdir, Y. Impact of land cover types on soil aggregate stability and erodibility. *Environ. Monit. Assess.* **2018**, *190*, 525. [CrossRef]
47. Schlüter, S.; Sammartino, S.; Koestel, J. Exploring the relationship between soil structure and soil functions via pore-scale imaging. *Geoderma* **2020**, *370*, 114370. [CrossRef]

48. Elmholt, S.; Schjønning, P.; Munkholm, L.J.; Debosz, K. Soil management effects on aggregate stability and biological binding. *Geoderma* **2008**, *144*, 455–467. [CrossRef]
49. Kristiansen, S.M.; Schjønning, P.; Thomsen, I.K.; Olesen, J.E.; Kristensen, K.; Christensen, B.T. Similarity of differently sized macroaggregates in arable soils of different texture. *Geoderma* **2006**, *137*, 147–154. [CrossRef]
50. Wu, H.; Wiesmeier, M.; Yu, Q.; Steffens, M.; Han, X.; Kögel–Knabner, I. Labile organic C and N mineralization of soil aggregate size classes in semiarid grasslands as affected by grazing management. *Biol. Fertil. Soils* **2012**, *48*, 305–313. [CrossRef]
51. Kaiser, M.; Walter, K.; Ellerbrock, R.H.; Sommer, M. Effect of land use and mineral characteristics on the organic carbon content, and the amount and composition of Napyrophosphate–soluble organic matter, in subsurface soils. *Eur. J. Soil Sci.* **2011**, *62*, 226–236. [CrossRef]
52. Blanco-Canqui, H.; Lal, R. Mechanism of carbon sequestration in soil aggregate. *Crit. Rev. Plant. Sci.* **2004**, *23*, 481–504. [CrossRef]
53. Li, Y.; Xiong, K.N.; Liu, Z.Q.; Li, K.P.; Luo, D. Distribution and influencing factors of soil organic carbon in a typical karst catchment undergoing natural restoration. *Catena* **2022**, *212*, 106078. [CrossRef]